On the structure of hyperbolic and near-parabolic dust streams

Eduard Pittich[1] **and Nina Solovaya**[2]

[1] **Slovak Academy of Sciences, Bratislava, Slovak Republic**
pittich@savba.sk

[2] **Lomonosov Moscow University, Moscow, Russia**
solov@sai.msu.ru

The only type of concentration of cometary dust with a reasonable probability of being detected by cosmic probes, are the dust tails emanating from passing comets. Essentially all the dust released from long-period comets leaves the solar system on hyperbolic orbits, because the radiation pressure limit is high.
For short-period comets the dynamical conditions for retention of emitted particles within the solar system are much more favorable. But those which remain in circum-solar orbits tend to disperse rather rapidly.
We present the results of an investigation of the evolution of dust streams produced by low-velocity emission from comets moving in near-parabolic and hyperbolic orbits. In order to get a clearer insight into the geometry and detectability of dust tails, some model computation have been performed.

1 Introduction

The Earth and its artificial satellites can encounter cometary dust debris only from comets whose perihelion distances q is less than 1 AU. Other cosmic probes flight behind the Earth's orbit can be penetrated by cometary dust ejected from comets with arbitrary perihelion distances.

On average two comets with $q < 1$ AU are observed per year. The average frequency of perihelion passages per year is 1.4 for long period comets (orbital period $P > 200$ yr), 0.1 for Halley type comets ($20 \text{ yr} < P < 200$ yr), 0.4 for Jupiter family comets ($4 \text{ yr} < P < 20$ yr), and 0.3 for comet Encke (Kresák, 1975). For one-apparition comets the average frequency of perihelion passage with $q < 1$ is 0.2 within 1900–1950 yr (Królikowska, et al., 2014). The short-period comets tend to liberate much less dust particles per revolution and their absolute brightness is much lower as in one-apparition comets.

The probability of penetrating the tail of a short-period comet is increased by their concentration to the ecliptic plane. But their low orbital inclinations at the same time imply lower impact velocities and fluxes, and hence higher requirements on the minimum detectable concentration of particles. Taking all this into account it can be inferred that the prospects of detecting dust particles from comets are much better for one-apparition comets.

The detectability of the direct dust tails has been discussed, and predictions provided, shortly after the first artificial cosmic probe flights. Already Poultney (1972, 1974) concluded that each passage of the Pioneer 8 and 9 detector would only be expected to yield one detected particle, but that other observable effects would be produced by the injection of the dust into the Earth's atmosphere.

2 Model computations

In order to get a clear insight into the geometry and detectability of cometary dust tails, some model computations have been performed by the authors. The figures in this paper show the orbital evolution of a dust stream produced by low-velocity emissions from two comets moving in a parabolic orbit of perihelion distance $q = 0.5$ AU, and, orbital inclination $i = 0^\circ$, and $i = 90^\circ$, respectively.

The colored dots in the figures indicated the positions of dust particles emitted from the comets by zero velocity started in the true anomaly of the comets $\nu = -150^\circ$ until $\nu = +150^\circ$, with the step $\Delta\nu = +30^\circ$, affected by the gravitational forces of the Sun and planets, the Poynting–Robertson effect, and the pressure of the solar wind (see e. g. Klačka and Pittich, 1994). For every value of ν the particle's position is plotted with the step of 30 days. The lower boundary of the particles mass $M = 10^{-11}$ kg. Each following particle has the mass one order of magnitude higher, up to 10^4 times the first value.

For our model we adopted Verniani's (1973) value of the particle density, $\rho = 800$ kg m^{-3}, obtained for faint radio meteors. This value, assuming spherical shape of a particle, corresponds to the particle's radius $s = 1.744 \times 10^{-5}$ m for $M = 10^{-11}$ kg, $s = 3.758 \times 10^{-5}$ m for $M = 10^{-10}$ kg, $s = 8.095 \times 10^{-5}$ m for $M = 10^{-9}$ kg, $s = 1.744 \times 10^{-4}$ m for $M = 10^{-8}$ kg, and $s = 3.758 \times 10^{-4}$ m for $M = 10^{-7}$ kg.

We traced orbital evolution of the comets and ejected particles using our numerical integration code with the integrator RA15 (Everhart, 1985). The masses and rectangular ecliptic coordinates and velocities of the planets for the numerical integrations of the equations of motion were taken from the JPL Horizons System[1] (Giorgini et al., 1996) on the date June 1, 2015.

[1] Web page: ssd.jpl.nasa.gov/?horizons

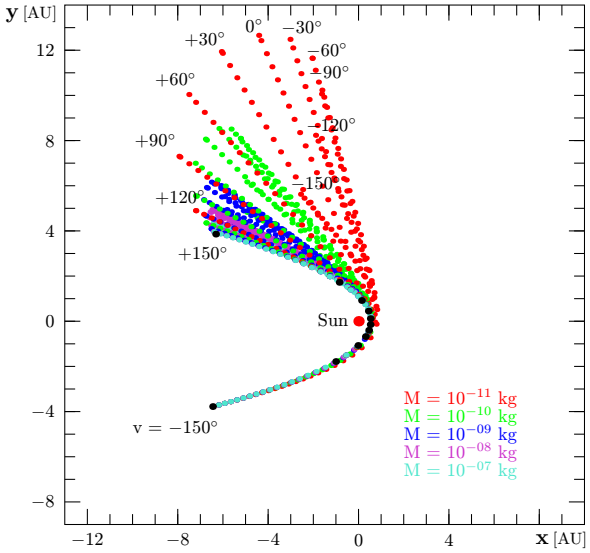

Figure 1 – Heliocentric ecliptic rectangular coordinates x, y of the particles with the mass M ejected from the comet with the zero velocity within the interval of $-150^\circ \le v \le +150^\circ$. The orbital elements of the comet: e = 1, q = 0.5 AU, i = 0°. Black dots are positions of the comet for used values of v.

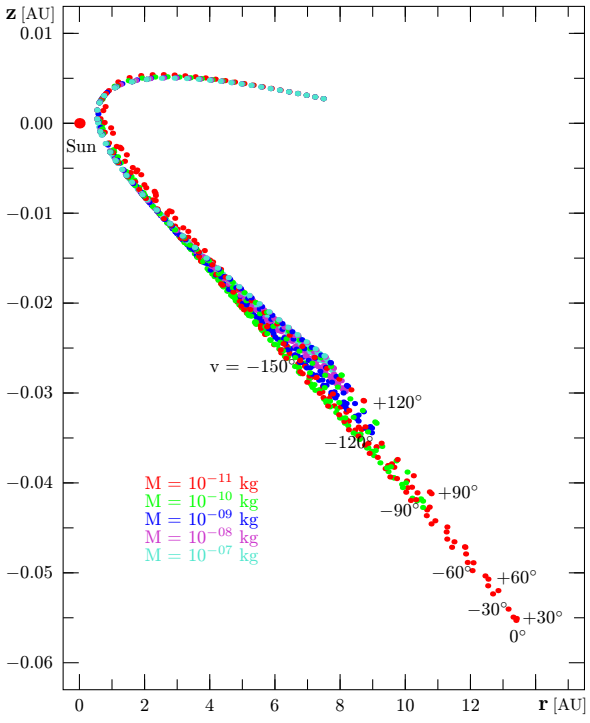

Figure 2 – Ecliptic altitude z versus heliocentric distance r of the particles with the mass M ejected from the comet with the zero velocity within the interval of $-150^\circ \le v \le +150^\circ$. The orbital elements of the comet: e = 1, q = 0.5 AU, i = 0°.

3 Results of orbital integration

The results obtained by numerical integration for the dust particles considered in our two models of cometary orbits with the perihelion passage T = June 1, 2015 are the particles ejected from the model comet with the inclination i = 0°. In this case the ecliptic plane is identical with the orbital plane of the comet. The last three figures contain information about the dynamical evolution of particles ejected from the comet with an orbital inclination i = 90°.

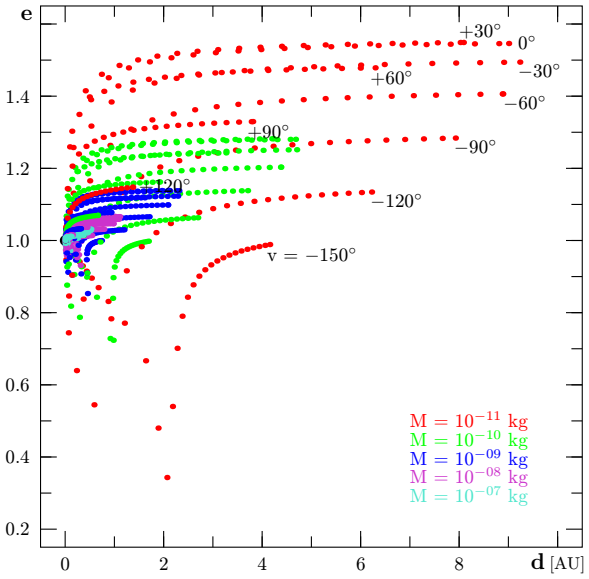

Figure 3 – Eccentricity e versus cometocentric distance d of the particles with the mass M ejected from the comet with the zero velocity within the interval of $-150^\circ \le v \le +150^\circ$. The orbital elements of the comet: e = 1, q = 0.5 AU, i = 0°.

Figure 1 displays the dispersion of particles in the comet's orbital plane toward to the comet within the investigated interval of v. At the comet's position for v = +150°, the dispersion of most particles is less than 2 AU. The smallest particles, with mass M = 10^{-11} kg, ejected at v = −150° are away from the comet about 4 AU and particles ejected at v = 0° are dispersed over at least 9 AU. The dispersion of the particles with mass 10 times greater than in the previous case is considerably less, about 2 AU and 4 AU, respectively.

Because the momentum of the particles is very little disturbed by planetary perturbations and non-gravitational forces within the investigated interval of v, their orbital inclinations are practically similar to the comet's inclination. This fact is illustrated in *Figure 2*. The maximum ecliptic altitude of some particles is –0.055 AU. They represent particles ejected at the perihelion of the comet.

The behavior of the eccentricities of the investigated particles versus their distance from the comet is presented in *Figure 3*. Most eccentricities of the model particles increase under the influence of non-gravitational forces, from 1 up to 1.55. The eccentricities of some particles, ejected until v = −90°, decrease within the first part of the investigated period. E. g. the highest value of the eccentricity, 0.35, was reached for the particle ejected at v = −150°, when it was 2 AU away from the comet.

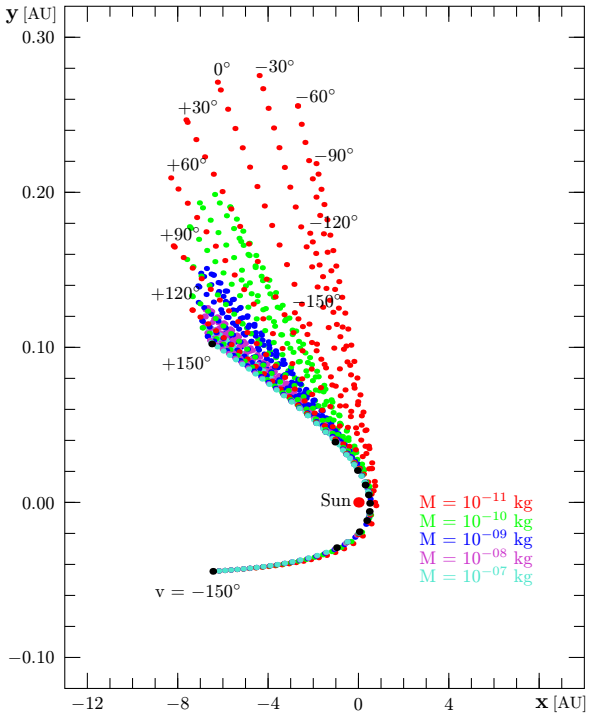

Figure 4 – Heliocentric ecliptic rectangular coordinates x, y of the particles with the mass M ejected from the comet with the zero velocity within the interval of $-150^\circ \le v \le +150^\circ$. The orbital elements of the comet: e = 1, q = 0.5 AU, i = 90°. Black dots are positions of the comet for used values of v.

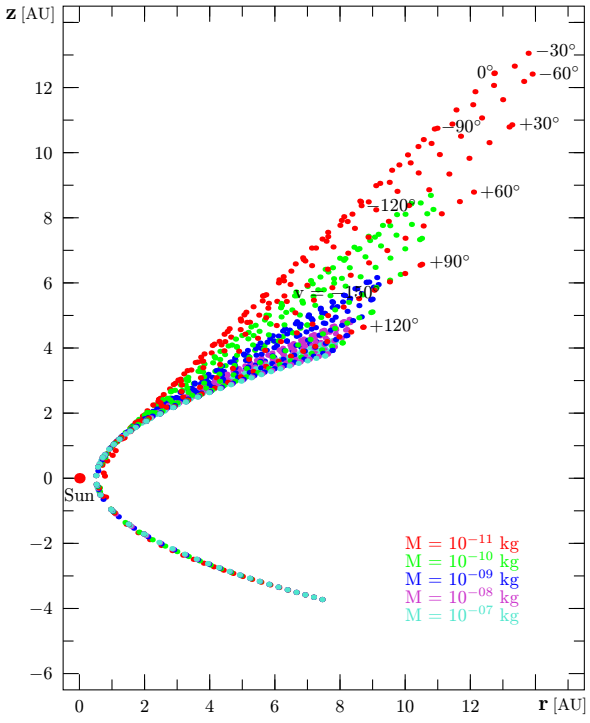

Figure 5 – Ecliptic altitude z versus heliocentric distance r of the particles with the mass M ejected from the comet with the zero velocity within the interval of $-150^\circ \le v \le +150^\circ$. The orbital elements of the comet: e = 1, q = 0.5 AU, i = 90°.

Similar results were obtained for the second comet's model with an orbital inclination of i = 90°. They are displayed in *Figures 4–6*. Of course in this case the comet's orbital plane is perpendicular to the ecliptic plane.

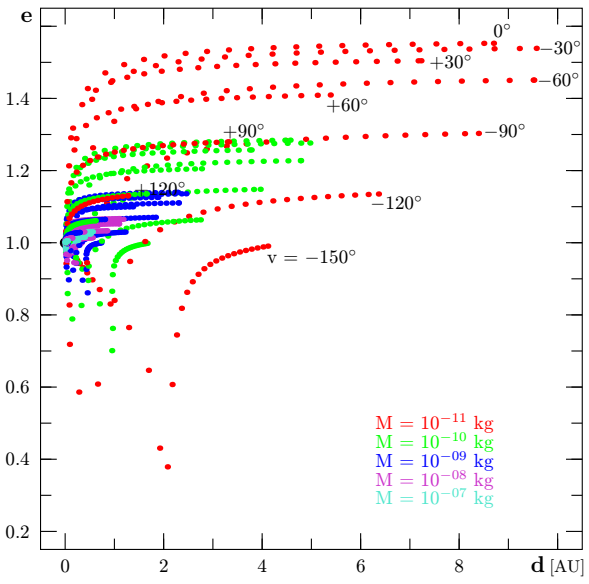

Figure 6 – Eccentricity e versus cometocentric distance d of the particles with the mass M ejected from the comet with the zero velocity within the interval of $-150^\circ \le v \le +150^\circ$. The orbital elements of the comet: e = 1, q = 0.5 AU, i = 90°.

For the same reason as in the previous model, the momentum of the particles is again disturbed negligibly by planetary perturbations and non-gravitational forces within the investigated interval of v. Therefore orbital inclinations of particles are very similar to the comet's inclination as we see in *Figure 4*. The maximum distance of some particles from the orbital plane of the comet is 0.28 AU for the particles ejected around the perihelion of the comet.

Figure 5 displays the ecliptic altitude z of the particles versus their heliocentric distances r within the investigated interval of the true anomaly v. In the first approximation, we can look at this figure as on the dispersion of particles toward the comet in its orbital plane. At the comet's position for $v = 150^\circ$, the dispersion of most particles is again less than 2 AU. The smallest particles, with mass $M = 10^{-11}$ kg, ejected at $v = -150^\circ$, are away from the comet about 2 AU, and those ejected at $v = -30^\circ$ at least 10 AU. The dispersion of particles with mass 10 times greater than in the previous case is less considerably, about 1 AU and 5 AU, respectively.

The behavior of the eccentricities of the investigated particles versus their distance from the comet is presented in *Figure 6*. It is very similar as in the case of the previous comet. The eccentricities for most of the model particles increase under the influence of non-gravitational forces, from 1 up to 1.55. The eccentricities of some particles, ejected until the true anomaly $v = -90^\circ$, decrease within the first part of the investigated period. E. g. the highest value of the eccentricity, 0.35, is reached for the particle ejected at the value of $v = -150^\circ$, when it was 2 AU away from the comet.

4 Conclusion

The spatial distribution of particles ejected with zero velocity from both comets with marginal orbital inclinations is very similar. Therefore, we can conclude that the resulting distribution of the investigated particles is more or less common for a parent parabolic comet with arbitrary orbital inclination. We can apply this result to all comets with near-parabolic, respective hyperbolic orbits, whose eccentricities are close to 1.

In spite of a number of simplifications involved, some interesting inferences are possible. Since the dust tail occupied a thin layer around the plane of a cometary orbit, the point of its crossing by a detector determines uniquely the size and time release of the particles encountered. The curvature and width of the dust tail rather than its length tends to increase during the apparition of the comet. The area occupied by the dust increases faster than the mass input. For the post perihelion arc the probability of encountering the tail is greater.

Essentially all the dust released from near-parabolic or hyperbolic comets leaves the solar system on hyperbolic orbits, because the radiation pressure limit is high. A similar conclusion can be made also for the same sources of dust streams in extrasolar planetary systems.

The structure of hyperbolic and near parabolic dust streams originating from one-apparition comets at their apparition near the Sun is similar. The width of such streams depends on the activity of a parent comet and its perihelion distance. For the detectability of such dust streams by space probes their origin and dynamical evolution must be taken into account.

A passage through the region of large particles and high particle concentration in a cometary dust stream would require a close approach to the comet and the crossing of its orbital plane at a suitable position angle. Such a situation would occur very rarely.

Acknowledgment

The authors thank the Local and Scientific organizing committee of the IMC 2015 for the conference in Mistelbach and its Proceedings 2015.

References

Everhart E. (1985). “An efficient integrator that used Gauss-Radau spacing”. In Carusi A. and Valsecchi G. B., editors, *Dynamic of Comets, their Origin and Evolution*, Reidel, Dordrecht, pages 185–202.

Giorgini J. D., Yeomans D. K., Chamberlin A. B., Chodas P. W., Jacobson R. A., Keesey M. S., Lieske J. H., Ostro S. J., Standish E. M., Wimberly R. N. (1996). “JPL’s on-line solar system data service”. *Bull. Am. Astron. Soc.*,**28**, 1158.

Klačka J., Pittich E. M. (1994). “Long-term orbital evolution of dust particles ejected from comet Encke”. *Planet. Space Sci.*,**42**, 109–112.

Kresák L. (1975). “The bias on the distribution of cometary orbits by observational selection”. *Bull. Astron. Inst.Czechoslov.*, **26**, 92–111.

Królikowska M., Sitarski G., Pittich E. M., Szutowicz S., Ziołkowski K., Rickman H., Gabryszewski R., Rickman B. (2014).“New catalogue of one-apparition comets discovered in the years 1901–1950. I. Comets from the Oort spike”. *Astronomy and Astrophysics*, **571**, A63, 1–19.

Poultney S. K. (1972). “Laser radar studies of upper atmosphere dust layers and the relation of temporary increases in dust to cometary micrometeoroid streams”. *Space Research*, **12**, 403–421.

Poultney S. K. (1972). “Times, locations and significance of cometary micrometeoroid influxes in the Earth's atmosphere”. *Space Research*, **14**, 707–708.